

The Electrochemical Behaviour of Brass in NaHSO₃ Solution Without and With Cl⁻

Q. Liu^{1,2}, H. Luo^{1,2}, C. F. Dong^{1,2,*}, K. Xiao^{1,2}, X. G. Li^{1,2}

¹ Corrosion and Protection Center, University of Science and Technology Beijing, Beijing, China

² Key Laboratory for Corrosion and Protection (MOE), Beijing, China

*E-mail: cfdong@ustb.edu.cn

Received: 12 September 2012 / Accepted: 9 October 2012 / Published: 1 November 2012

The electrochemical behaviour of brass in NaHSO₃ solution without and with Cl⁻ was investigated by potentiodynamic polarization and cyclic voltammetry techniques. The results indicated brass dissolution was accelerated with HSO₃⁻ concentration increasing. And the first stable region in polarization curves was attributed to adsorbed layers, while the other to the formation of copper oxides. In the mixed solution containing HSO₃⁻ and Cl⁻, when the potential is under -0.2 V_{SCE}, HSO₃⁻, the dominant factor influencing the corrosion behaviour of brass, inclines to make brass stable; while Cl⁻ becomes the leading aspect above -0.2 V_{SCE} by destroying protective layers.

Keywords: Brass, Polarization, Cyclic Voltammetry, SEM

1. INTRODUCTION

Considering the wide applications of brass alloys in fabricating structures and components exposed to various environments, their electrochemical behaviour is an increasingly essential issue, calling for more attention. The electrochemical behaviour of Cu alloys has been studied extensively, especially in the solution containing Cl⁻ [1-7]. It is demonstrated that copper dissolves via a two-step reaction mechanism in a solution containing Cl⁻ [1-4]. Firstly, Cu quickly transforms to CuCl_{ads}, which adsorbs on the electrode surface [5,6]. Then CuCl_{ads} further transforms to CuCl₂⁻, which determines the dissolution process of Cu alloys [6,7]. For the copper alloys containing Zn, the element zinc provides a cathodic protection to copper through a replacement reaction, leading to the re-deposition of Cu and the dissolution of Zn as ZnCl₄²⁻ [8]. The research [9] for the electrochemical behaviour of brass alloy in acid solutions showed that Zn dissolution occurred at more negative potentials with the appearance of two anodic peaks in the cyclic voltammetry curve, which corresponded to the formation of ZnO and

Zn(II), respectively. With the positive shift of potential, current increased abruptly as a result of a simultaneous dissolution of both copper and zinc. And two more anodic peaks were observed, corresponding to the formation of $\text{Cu}_2\text{O}/\text{CuCl}$ and CuO [1], respectively, at even higher potential.

On the other hand, with the environmental pollution due to the speedy development of the industry, SO_2 is becoming an important factor influencing the performance and the service life of mechanical components by considerable corrosion damage [10-12]. Many studies have been worked on about copper and its alloys in the solution containing SO_4^{2-} . Fonseca [13] suggested that SO_4^{2-} ions could promote the film formation in the passive range and increase the amount of soluble Cu species. It was found that a transition region appeared in the cyclic voltammetry due to the formation of adsorbed species, like $\text{Cu}(\text{SO}_4)_{\text{ads}}^{2-}$, or $\text{Cu}(\text{OH})_{\text{ads}}^-$ on the sample surface [14]. Moreover, according to the obtained curves, the anodic current densities were enhanced with the increase of Zn content. In acid chloride and sulphate media, O_2 mainly reduced to H_2O directly as a cathodic reaction [15,16].

On the other hand, the fact that SO_2 accelerates atmospheric corrosion is primarily ascribed to the strong depolarizing agent H_2SO_3 generated after SO_2 being adsorbed in water. So, the NaHSO_3 solution was employed to simulate the industrial environments with SO_2 . There are limited investigations concerning the effect of HSO_3^- on the corrosion and electrochemical behaviour of brass, less mention on the cooperation of HSO_3^- and Cl^- . The aim of this work is to investigate the electrochemical behaviour of brass in NaHSO_3 solution without and with Cl^- by polarization curves, cyclic voltammetry (CV) and scanning electron microscopy (SEM). It is anticipated that this research would provide the essential insight for the future protection of brass in the environment containing both SO_2 and Cl^- , like the industrial district in the offshore area.

2. EXPERIMENTAL

2.1 Preparation of samples and solutions

The brass samples, with the dimension of 10 mm \times 10 mm \times 3 mm, were used and the chemical composition was Cu (61.56 wt. %), Zn (38.43 wt. %) with Pb balance. After being welded to copper wire to assure the electric connection for electrochemical measurement, the samples were embedded into epoxy resin, leaving an exposed area of 1 cm². Prior to electrochemical measurements, samples were sequentially ground with silicon carbide emery paper up to 2000 grit, then rinsed with deionised water and alcohol and dried by cool air.

Analytical-grade NaHSO_3 , NaCl and triply distilled water were used for preparing solutions. The concentrations used in this experiment were as follows: 0.01 M, 0.05 M, 0.1 M, 0.2 M and 0.4 M NaHSO_3 with/without 0.1 M NaCl .

2.2 Electrochemical measurements

A conventional three-electrode cell arrangement was used for electrochemical measurements, with a saturated calomel electrode (SCE) as the reference electrode and a platinum plate as the counter

electrode. Electrochemical measurements were carried out with Princeton Applied Research-VMP3 electrochemical system at 25 °C.

Polarization measurements were carried out by shifting the potential from -0.6 V (vs. open circuit potential-OCP) to +0.6 V_{SCE} with a scan rate of 1 mV/s. For CV measurements, a potential sweep from -1.0 V_{SCE} to +0.6 V_{SCE} and then back to -1.0 V_{SCE} with a scan rate of 10 mV/s was used. After polarization measurements, surface morphologies of samples were observed by SEM. Each experiment was performed in a freshly prepared solution and with a newly ground electrode surface.

3. RESULTS AND DISCUSSION

3.1 The electrochemical behaviour of brass in NaHSO₃ solution

3.1.1 The potentiodynamic polarization of brass

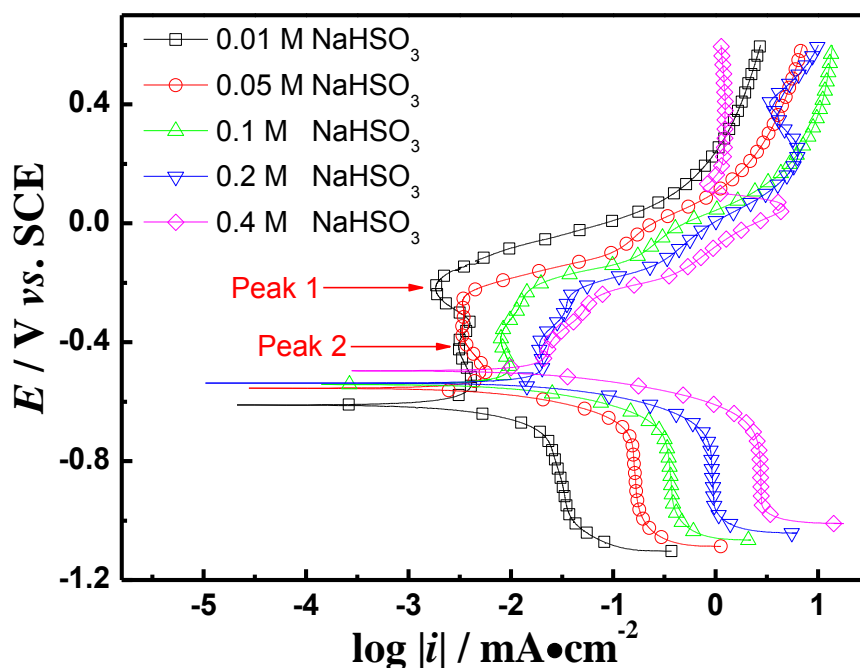


Figure 1. Polarization curves of brass in different concentrations of NaHSO₃ solution, scan rate: 1 mV/s.

Fig. 1 shows the polarization curves of brass in NaHSO₃ solutions. It is apparent that the corrosion potential (E_{corr}) shifts to more noble value with the increase of NaHSO₃ concentration. The anodic current density and the cathodic current density increase greatly, indicating that both the anodic and cathodic reactions are accelerated by adding HSO₃⁻ ions in the solution.

As is shown in the Fig.1, an apparently stable cathodic current density at approximate -950 mV_{SCE} to -700 mV_{SCE}, proves the involvement of diffusion process. In this region, dissolved oxygen is

reduced directly to H₂O via 4-electron pathway [15,16]. This is the case that the cathodic process is totally controlled by diffusion process, which prevents linear extrapolation of cathodic curves.



For the anodic process, in the polarization curves obtained in the 0.01 M NaHSO₃ solution, two anodic current density peaks can be observed in the potential range from -0.55 V_{SCE} to -0.2 V_{SCE}, as shown in Fig. 1. One peak is at about -0.22 V_{SCE} (Peak 1) with the value of 1.9 μA•cm⁻² and the other at about -0.41 V_{SCE} (Peak 2) with 3.1 μA•cm⁻². And the values at peaks just slightly deviate from the average current density (about 3.2 μA•cm⁻²) in this region, revealing a passivation phenomenon. On the other hand, the fluctuant current densities indicate that there is a competition of two kinds of reaction: accelerating and inhibiting the metal dissolution rate, respectively. Whenever the former aspect is larger than the later aspect, the current density will increase. While when the two rates equal to each other, the current density will stay stable. When the potential overtakes -0.2 V_{SCE}, the anodic current density increases quickly, revealing that the metal dissolution rate has been sped up a lot and the inhibitive reaction can be negligible.

With the HSO₃⁻ concentration increasing from 0.05 M to 0.4 M, there are also two anodic current density peaks appearing on each curve between -0.55 V_{SCE} and -0.2 V_{SCE}, respectively. But both these two current density peaks and the average current density in this region increase with the HSO₃⁻ concentration. From another point of view, this indicates that the reaction inhibiting the metal dissolution rate is weakening by the increasing HSO₃⁻ concentration. Moreover, the peak current density at about -0.2 V_{SCE} increases more than that at -0.4 V_{SCE}, indicating that this stable range of current density is gradually transforming into an active region. When the potential surpasses -0.2 V_{SCE}, the anodic current density increases quickly. However, as for the curves obtained in the 0.2 M NaHSO₃ solution, the current density begins to drop at 0.24 V_{SCE} though followed by an increase at 0.4 V_{SCE}; while for 0.4 M solution, the current density begins to decrease at 0.05 V_{SCE}, and then keeps stable at 1.2 mA•cm⁻² after 0.12 V_{SCE}. As has been discuss above, it can be concluded that in solutions with low and high HSO₃⁻ concentration, brass shows different behaviour.

3.1.2 CV curves analysis

In order to further clarify the HSO₃⁻ effect on brass during the polarization process, CV were carried out on brass in the solution with different NaHSO₃ concentrations at a scan rate of 10 mV/s (as is shown in Fig. 2). And parts of the CV curves in different potential regions are compared in Fig.3.

Fig. 2(a) and 2(b) show the CV curves of brass in 0.01 M and 0.05 M NaHSO₃ solution, respectively. They are somewhat similar and resemble with the CV curve of Cu38Zn in 0.05 M Na₂SO₄ solution [14]. The potential scan was started from -1.0 V_{SCE}. After setting up the positive-going sweep, the cathodic current decreases as the potential shifts positively.

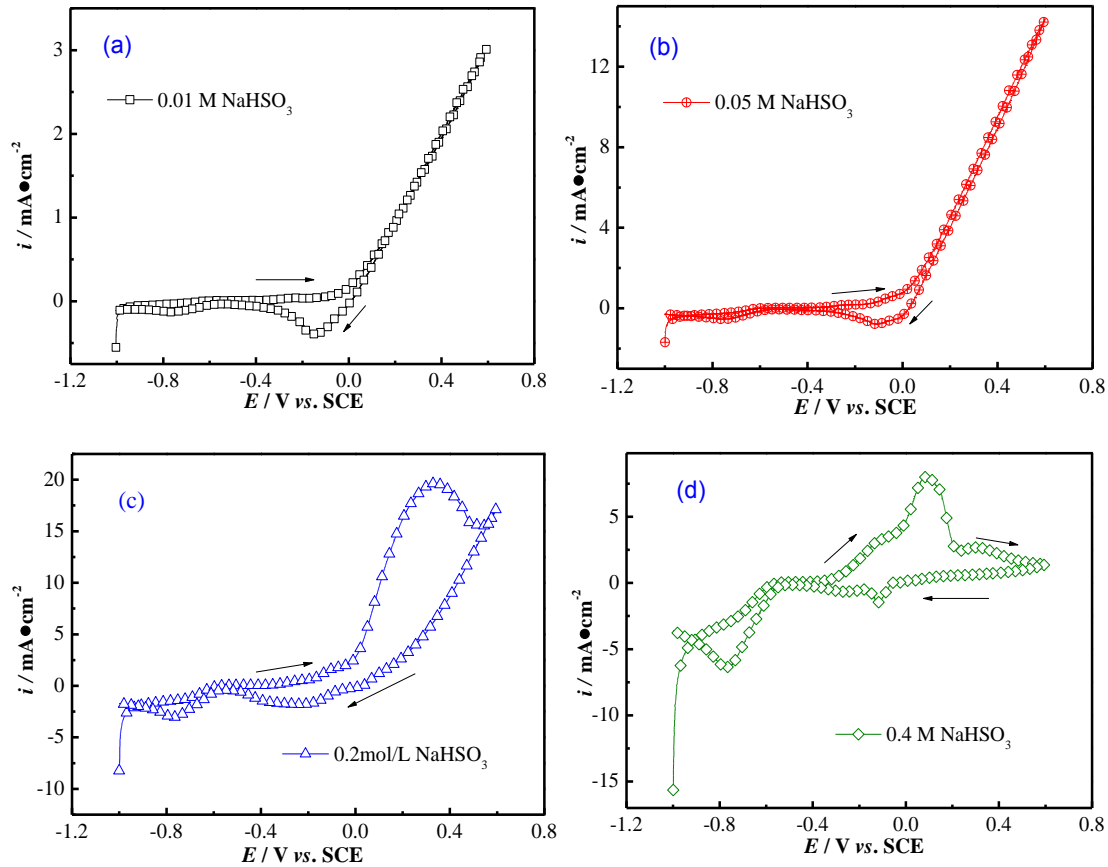
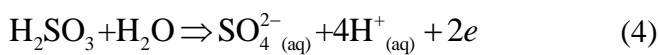
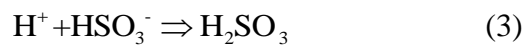


Figure 2. The CV curves obtained in the various concentration of NaHSO₃ solution, scan rate: 10mV/s; (a) 0.01 M; (b) 0.05 M; (c) 0.2 M; (d) 0.4 M.

Then a transition region extending up to 0 V_{SCE}, corresponding to the current stable region appeared in the polarization curve in Fig. 1 before the active dissolution of brass occurs. This can be probably ascribed firstly to the formation of adsorbed species Cu (HSO₃)_{ads}⁻ on the electrode surface via the reaction:



However, the current density starts to increase due to the dissolution of the absorption layer Cu (HSO₃)_{ads}⁻ since HSO₃⁻ can be oxidized to SO₄²⁻ with the increase of polarization potential according to Eq.3 and Eq.4 [17].

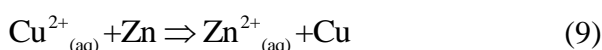
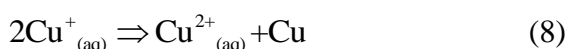
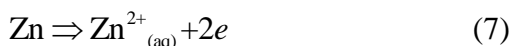


Therefore, the original absorbed HSO_3^- ions on the sample surface can be replaced by SO_4^{2-} ions, leading to the appearance of the $\text{Cu}(\text{SO}_4)_{\text{ads}}^{2-}$ layer (according to Eq.5 [14]), which decreases current density.



The formation of this absorption layer corresponds to Peak 2 in the passive region at about -0.21 V_{SCE} in the polarization curves.

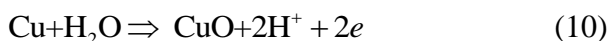
$\text{Cu}(\text{HSO}_3)_{\text{ads}}^-$ or $\text{Cu}(\text{SO}_4)_{\text{ads}}^{2-}$ species represent the adsorbed intermediate products for active dissolution. They compete for the adsorption sites at the metal surface, which may promote dissolution or passivation with increasing potential [18]. When the potential over 0 V_{SCE} , the anodic current starts to increase, which can be ascribed to the dissolution process of the absorbed layer and the formation of $\text{Cu}_2(\text{SO}_4)_{\text{(aq.)}}$ (Eq.6) [19] and a disproportionation of cuprous ion and the replacement reaction between Zinc and copper ions (Eqs. 7~9).



Cu^{2+} is further replaced by Zinc to redeposit on the substrate, which increases the cathodic area, resulting in the formation of active galvanic couples and the increase in the corrosion rate of brass [18].

The reverse scan shows a cathodic peak 1 (in Fig.3(b)) recorded at -0.15 V_{SCE} , which is due to the reduction of copper ions. And another cathodic peak at -0.76 V_{SCE} corresponds to the electro-reduction of the dissolved oxygen.

The CV for brass in 0.2 M NaHSO_3 solution is shown in Fig. 2(c). The current density shoulder 1'', corresponding to the formation of $\text{Cu}(\text{SO}_4)_{\text{ads}}^{2-}$, is still higher than that in lower NaHSO_3 concentration solutions. This may be due to the acceleration of the oxidation reaction of HSO_3^- , leading to an approximate H_2SO_4 surrounding on the sample surface and an increase of the solution aggressiveness. Due to the dissolution of absorbed layer, the current increases sharply until the polarization potential shifts up to 0.336 V_{SCE} (peak 2'' in Fig. 3a), at which CuO begins to form though Eq.10 [20] and leads to a decrease in the current.



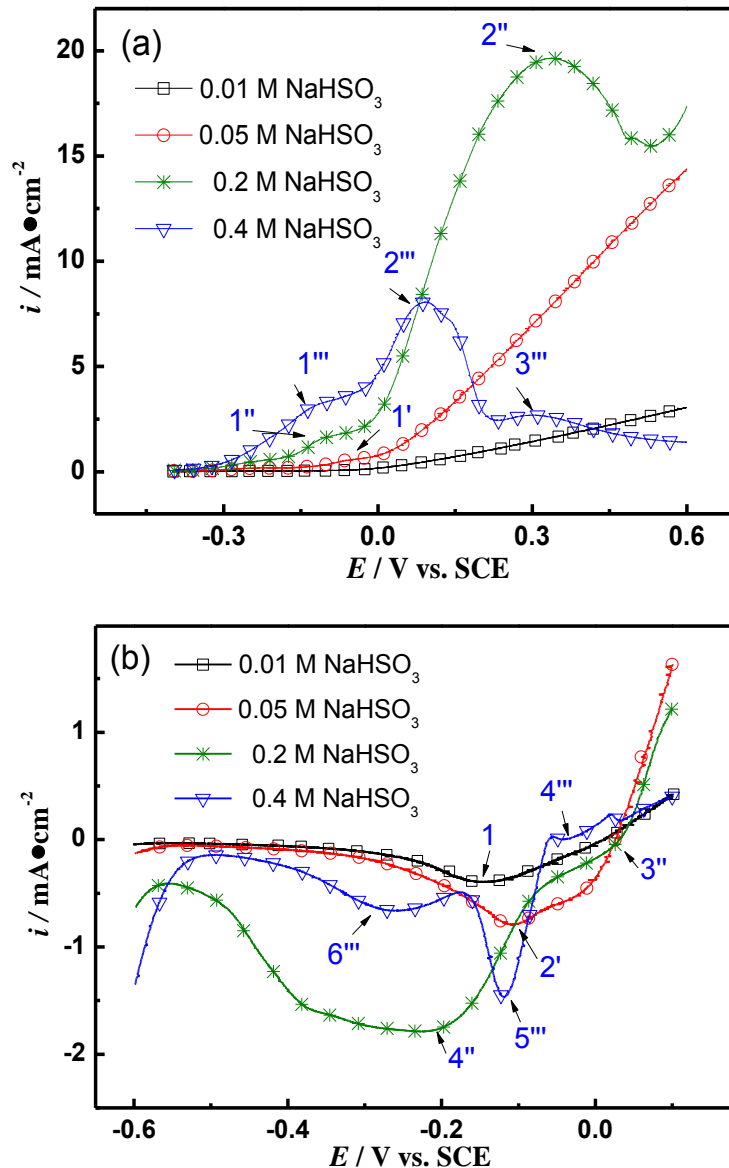


Figure 3. Part of the CV curves obtained in various concentrations of NaHSO₃ solution, 10mV/s: (a) - 0.4 V ~ 0.6 V in the positive scan; (B) 0.1 V ~ -0.6 V in the reverse scan.

Therefore, the cathodic peak 3'' (in Fig. 3(b)) recorded at 0.03 V_{SCE} is due to the reduction of CuO, while another cathodic peak at -0.2 V_{SCE} is related to the reduction of copper ions. Cathodic peak, corresponding to the electro-reduction of the dissolved oxygen, is at -0.76 V_{SCE}.

As for the CV curve obtained in 0.4 M NaHSO₃ solution, still the current density shoulder 1''' is attributable to Cu(SO₄)_(aq)²⁻. A new anodic current density peak 2''' (shown in Fig. 3b) appears on the obtained curve except peak 3'', which is due to CuO. The formation of Cu₂O on the sample surface can be an explanation for the peak 2'''. The reaction is shown in Eq.11 [20].



In this case, the peak 4''', 5''' and 6''' in the reverse scan (as shown in Fig.3(b)) are attributed to the reduction of CuO, Cu₂O and copper ions respectively.

It is concluded that brass is inclined to be more active with the increase of HSO₃⁻ concentration in the low potential range. On the other hand, the formation of CuO and Cu₂O at the high potential range in the solution with high HSO₃⁻ concentration greatly enhances the corrosion resistance of brass, which results in the relatively stable current density even with the increase of the applied potential. Therefore, brass can be protected either because of the absorbed layer or the copper oxides.

3.2 The electrochemical behaviour of brass in mixed solution with Cl⁻ and HSO₃⁻

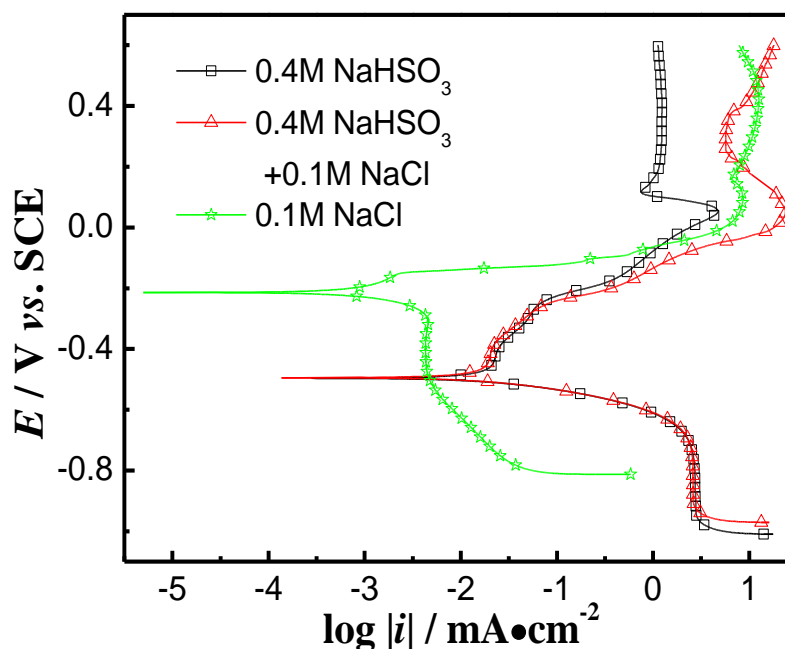


Figure 4. Polarization curves of brass in different electrolytes, scan rate: 1 mV/s.

Fig.4 shows the polarization curves of brass obtained in mixed solution containing 0.1 M NaCl + 0.4 M NaHSO₃, 0.1 M NaCl solution and 0.4 M NaHSO₃ solution, respectively. With the existence of HSO₃⁻ ions in the solution, obviously, E_{corr} shifts to a more negative value and i_{corr} (about 10.4 $\mu\text{A}\cdot\text{cm}^{-2}$) is 20 times higher than that in the solution without HSO₃⁻ ions (about 0.6 $\mu\text{A}\cdot\text{cm}^{-2}$), which points out the dissolution of brass was accelerated by adding HSO₃⁻ ions.

It is worth noting that the similar polarization character is observed for brass in NaHSO₃ solutions with and without Cl⁻ when the potential is below -0.2 V_{SCE} [1]. This suggests that, in this potential range, the corrosion mechanism of brass in the mixed solution is the same as that in NaHSO₃ solution. In this case, HSO₃⁻ is the main factor influencing the electrochemical behaviour of brass.

On the other hand, when the potential exceeds -0.2 V_{SCE}, obviously, the current density obtained in the solution with Cl⁻ becomes bigger and bigger than that in the solution without Cl⁻. This phenomenon indicates that Cl⁻ has greatly boosted the dissolution rate[21,22]. Moreover, noticeably,

the stable region of current density at high potential in the 0.4 M HSO_3^- solution disappears in the presence of Cl^- . This indicates that Cl^- begins to involve in the polarization process in the mixed solution containing both HSO_3^- and Cl^- , and has more influence than HSO_3^- in high potential region.

As mentioned above, the presence of HSO_3^- accelerates corrosion rate of brass, while the existence of aggressive Cl^- can break down the protective film formed on the sample surface[23]. Therefore, in the mixed solution containing HSO_3^- and Cl^- , HSO_3^- (or Cl^-) is the dominant factor when the potential below (or above) $-0.2 \text{ V}_{\text{SCE}}$.

3.2.1 HSO_3^- as the main factor in mixed solution containing HSO_3^- and Cl^-

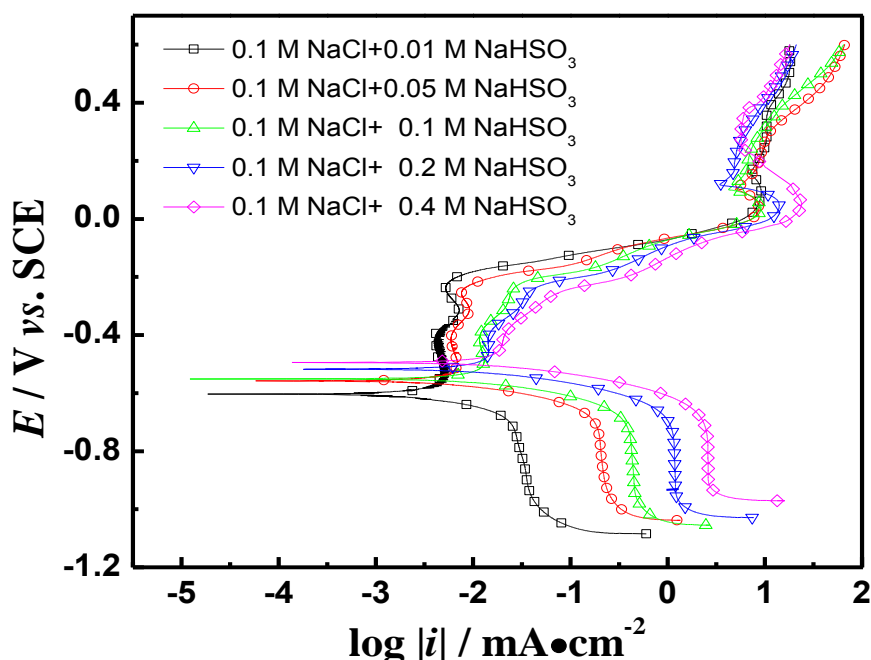


Figure 5. Polarization curves of brass in different concentration of NaHSO_3 solution with 0.1 M NaCl , scan rate: 1 mV/s.

Fig.5 shows the polarization curves of brass obtained in various NaHSO_3 solutions with 0.1 M Cl^- . Compared with Fig.1, it indicates that in each concentration of NaHSO_3 solution, similar polarization curves of brass are obtained with and without Cl^- when the potential is below $-0.2 \text{ V}_{\text{SCE}}$.

Fig.6 shows the electrochemical parameters, such as E_{corr} , i_{corr} , the diffusion-limited current density (i_L), and the current density at $0.4 \text{ V}_{\text{SCE}}$ (i_a), obtained from the curves in Fig.1 and Fig.5. It can be seen clearly that with the increase of HSO_3^- concentration, E_{corr} shifts to negative values in Fig.6 (a), which means E_{corr} becomes nobler with HSO_3^- concentration. It changes from $-612 \text{ mV}_{\text{SCE}}$ to $-496 \text{ mV}_{\text{SCE}}$ in the NaHSO_3 solution, while from $-604 \text{ mV}_{\text{SCE}}$ to $-495 \text{ mV}_{\text{SCE}}$ in the mixed solution. Obviously, the corresponding data are pretty much the same, which reflects that the addition of Cl^- does not affect E_{corr} much.

The same phenomenon happens to i_{corr} and i_{L} as well, as seen in Fig.6(b) and(c). Though they increased with the HSO_3^- concentration, very corresponding parameter value obtained in the mixed solution is pretty much the same as that obtained in the NaHSO_3 solution. All has been stated above confirms that HSO_3^- is the dominant factor instead of Cl^- when the potential is below $-0.2 \text{ V}_{\text{SCE}}$ in the mix solution with HSO_3^- and Cl^- . The specific influence of HSO_3^- on the corrosion behaviour of brass can be referred in the 3.1.

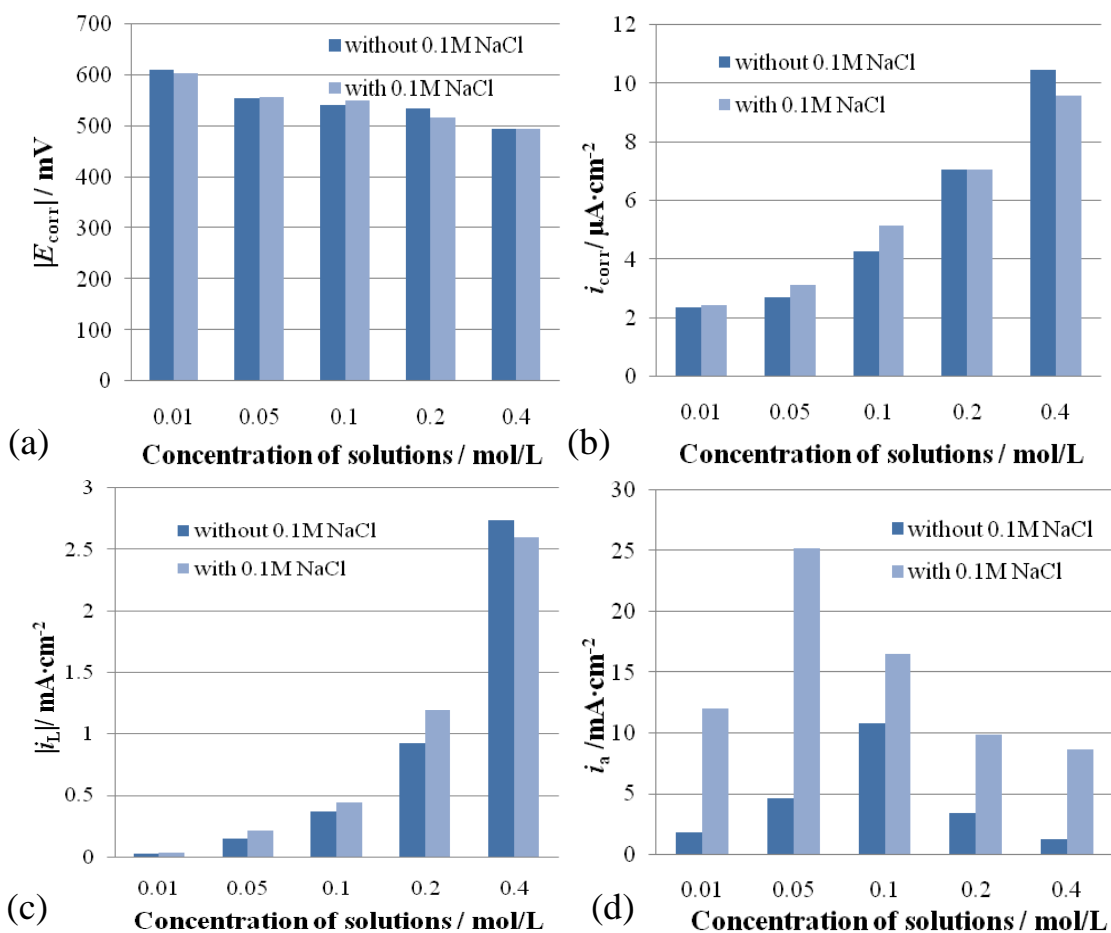


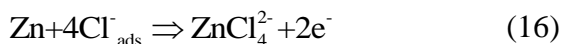
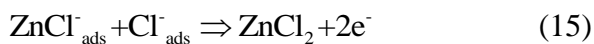
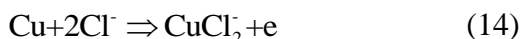
Figure 6. Comparison of electrochemical several corresponding parameters obtained in NaHSO_3 solution and in the mixed solution. (a) E_{corr} ; (b) i_{corr} ; (c) i_{L} ; (d) i_{a} .

3.2.2 Cl^- as the main factor in mixed solution containing HSO_3^- and Cl^-

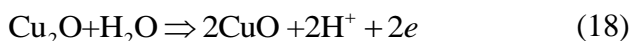
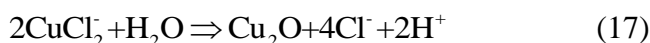
As stated above, Cl^- is the major factor influencing the corrosion behaviour when the applied potential overtakes $-0.2 \text{ V}_{\text{SCE}}$. The most direct evidence is the noticeable increase in i_{a} in the solution with Cl^- , as can be seen in Fig.6. For instance, i_{a} were $1.8 \text{ mA}\cdot\text{cm}^{-2}$ and $12.0 \text{ mA}\cdot\text{cm}^{-2}$, respectively, in the 0.1 M NaHSO_3 solution and in the solution with Cl^- .

It is noticed that when the polarization potential surpassed $-0.2 \text{ V}_{\text{SCE}}$, the anodic current density begin to increase sharply, indicating that protective layer $\text{Cu}(\text{SO}_4)_{\text{ads}}^{2-}$ on the sample surface began to

dissolve (according to Eq.6) as well as the replacement reaction between Cu and Zn (according to Eqs. 7 ~ 9) as has been stated in 3.1.2. Moreover, the dissolution of Cu and $\text{ZnCl}_{\text{ads}}^-$ also results in the current density increasing, according to the following reactions [8, 9]:

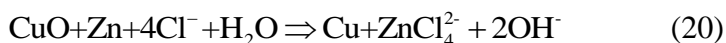
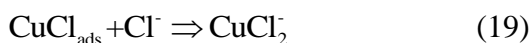


When the potential reaches about 0 V_{SCE}, the increase in current density begins to slow down, mainly due to the formation of Cu₂O and CuO on the electrode surface according to Eq. 17[24] and Eq.18 [20].



Moreover, since the solubility of $\text{CuCl}_{\text{ads}}^-$ is low, a porous film of $\text{CuCl}_{\text{ads}}^-$ can be formed after $\text{CuCl}_{\text{ads}}^-$ precipitating at the surface of the electrode [25]. Eventually, the current density decreases at 0.09 V_{SCE}.

However, these protective products would transfer to soluble complex CuCl_2^- and ZnCl_4^{2-} (according to Eq.19 and 20 [8]), leading to an inclination of increasing in the current density. Consequently, the simultaneous formation and dissolution of protective products result in the “S” shape in the anodic polarization curve at high potential region.



Considering what has been discussed above, the existence of Cl^- leads to the inclination of formation of soluble products, like CuCl_2^- and ZnCl_4^{2-} , to take place of protective products, like $\text{CuCl}_{\text{ads}}^-$ and CuO on the surface. Therefore, Cl^- accelerating the dissolution rate of brass is mainly by destroying protective layer on the sample.

3.3 SEM and EDS results

Fig.7 and Fig.8 provide the surface SEM images of brass after polarization in the NaHSO₃ solution and in the mixed solution. Apparently, there are some hollow parts appearing on the surface, which is attributed to the preferential dissolution of zinc in brass. This corresponds with the

explanation of the electrochemical behaviour of brass in the electrochemical measurements. Moreover, as can be seen, relatively minor corrosion is observed due to the formation of protective film on the electrode surface in the NaHSO_3 solution without Cl^- . However, corrosion products with irregular shapes are obtained in the mixed solution, reflecting the strong aggressive effect of Cl^- on protective film, which verifies the conclusion in the 3.2.2 part.

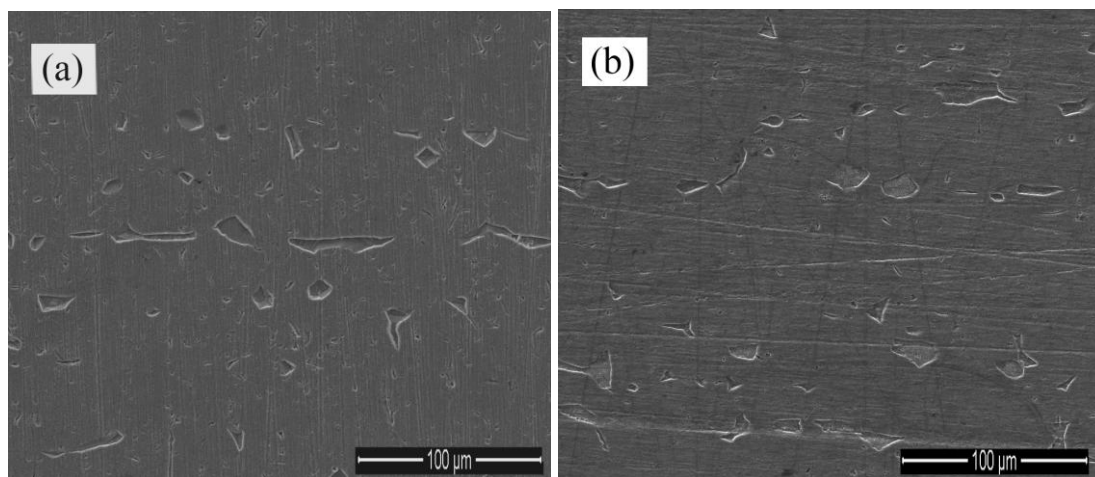


Figure 7. SEM images of brass after polarization in NaHSO_3 solution (a) 0.01 M NaHSO_3 ; (b) 0.4 M NaHSO_3 .

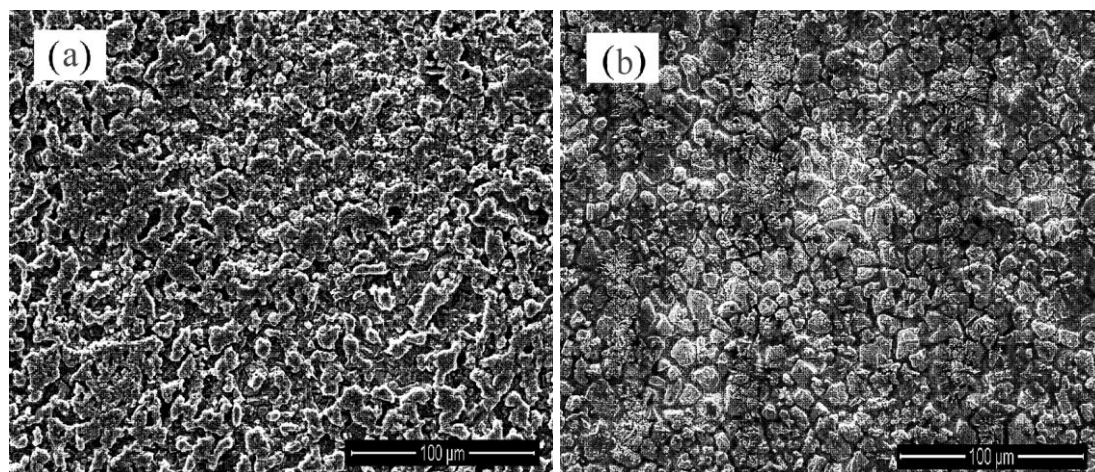


Figure 8. SEM images of brass after polarization in NaCl solution without and with NaHSO_3 : (a) 0.1 M Cl^- + 0.01 M HSO_3^- ; (b) 0.1 M Cl^- + 0.4 M HSO_3^- .

Fig. 9 shows the EDX analyses of the corrosion products on the samples obtained in the solution either with HSO_3^- or not. Compared with Fig.9(a), the existence of O element in Fig.9(b) reveals that there are oxides forming on the sample just as has been discussed above. However, this protective layer can be break down by Cl^- , resulting in the further dissolution of sample. Moreover, the contents of Zn are only approximate 24 wt% and 10 wt% in corrosion products in the solution with or

without HSO_3^- , respectively, which is less than its original content in brass (about 38%), revealing the dezincification in polarization process.

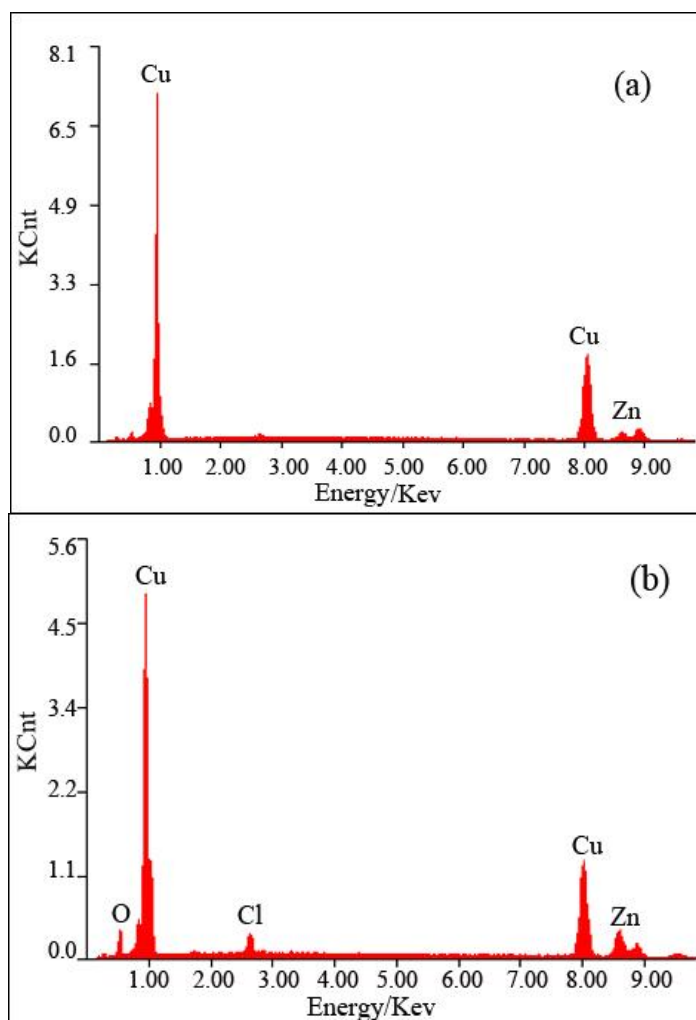


Figure 9. EDX analysis of the corrosion products of brass after polarization in: (a) 0.1 M NaCl; (b) 0.2 M NaHSO_3 + 0.1M NaCl.

4. CONCLUSIONS

In the NaHSO_3 solution, the corrosion rate of brass increases with HSO_3^- concentration increasing. However, HSO_3^- inclines to lead brass to a stable state either in low concentration of or in higher concentration of HSO_3^- . The first passive region is attributed to the adsorbed layer consisting of $\text{Cu}(\text{HSO}_3)^-_{\text{ads}}$ or $\text{Cu}(\text{SO}_4)^{2-}_{\text{ads}}$. And the appearance of another stable region at more noble potentials can be ascribed to the formation of CuO or Cu_2O layer.

In the mixed solution containing both HSO_3^- and Cl^- , there is a threshold potential value, at approximate $-0.2 \text{ V}_{\text{SCE}}$, to separate the main factor influencing the anodic dissolution of brass. When the potential is below $-0.2 \text{ V}_{\text{SCE}}$, HSO_3^- is the dominant factor; whereas when the potential is over $-0.2 \text{ V}_{\text{SCE}}$. The Cl^- exits as a major factor, leading to the increase in the corrosion current density. Moreover, with the existence of Cl^- , no matter HSO_3^- concentration high or low, the stable region at more noble

potential disappears. This is ascribed that Cl^- can destroy and inhibit the formation of protective film on the sample.

ACKNOWLEDGMENTS

This work is supported by the Fundamental Research Funds for the Central Universities (No. FRF-TP-11-006B) and the National Natural Science Foundation of China (No.51131005, 50771020)

References

1. K. Xiao, C. F. Dong, H. Luo, Q. Liu, X. G. Li, *Int. J. Electrochem. Sci.* 7(2012) 7503.
2. A.M. Alfantazi, T.M. Ahmed and D. Tromans, *Mater.Des.* 30(2009) 2425.
3. Z. Mountassir, A. Sghiri, *Corros.Sci.* 49(2007) 1350.
4. W.A.Badawy, S.S. El-Egamy and A.S. El-Azab, *Corros.Sci.* 37(1995) 1969.
5. M. Scendo, *Corros.Sci.* 47(2005) 2778.
6. M. Scendo, *Corros.Sci.* 47(2005) 1738.
7. G. Bianchi, P. Longhi, *Corros.Sci.* 13(1973) 853.
8. M. Kabasakaloglu, T.Kiyak, O.Sendil and A.Asan, *Appl.Surf.Sci.* 193(2002) 167.
9. S. S. Abd. El-Reuim, F. H.Assaf, A.El-Sayed and A. M. Zaky, *Br.Corros.J.* 1995(30) 297.
10. M. Watanabe, Y. Higashi and T. Ichino, *J. Electrochem.Soc.* 150(2003) B37.
11. R.B.Comizzoli, R.P.Frankenthal, P.C.Milner and J.D.Sinclair, *Science.* 234(1986) 340.
12. Z.Y.Chen, C.Y.Leygraf, D.Y.Persson and S.Y.Zakipour, 61(2005) 1022.
13. I.T.E.Fonseca, A.C.S. Marin and A.C. Sá, *Electrochim.Acta.* 37(1992) 2541.
14. K.M. Ismail, R.M. Elsherif and W.A. Badawy, *Electrochim.Acta.* 49(2004)5151.
15. K.Balakrishnan, V.K. Venkatesan, *Electrochim.Acta.* 24(1979) 131.
16. M.A. Amin, K.F. Khaled, *Corros.Sci.* 52(2010) 1194.
17. J.G.Speight, Lange's Handbook of Chemistry (16th Edition), McGraw-Hill.
18. V.P. Parkhutik, J.M. Albella, and J.M. Martinez-Duarte, 1992, Plenum Press: New York.
19. K.M.Ismail, A.M. Fathi and W.A. Badawy, *Corrosion.* 60(2004) 795.
20. M.Pourbaix, NACE, Houston, TX, 1974.
21. H. Luo, C.F. Dong, X.G. Li, K. Xiao, *Electrochim.Acta.* 64(2012)211.
22. J.H.Wang, C.C.Siu, Z.Szklarska-Smialowska. *Corrosion.* 44 (1988)732.
23. C.-O.A. Olsson, D. Landolt, *Electrochim.Acta.* 48(2003)1093.
24. A.L. Bacarella, J.C. Griess, *J. Electrochem.Soc.* 120(1973)459.
25. F.Crundwell, *Electrochim.Acta.* 36(1991) 2135.